Enhanced photocatalytic degradation of diethyl phthalate using Zn doped rutile TiO_2

Pooja Singla, O P Pandey & K Singh*

School of Physics and Materials Science, Thapar University, Patiala 147 004, India

A simple, room temperature sol gel synthesis approach has been made to obtain undoped and Zn doped TiO_2 samples using titanium tetraisopropoxide and zinc acetate as precursors. The synthesized samples are predominantly in rutile phase which are rarely reported at the calcination temperature of 450 °C. The samples are characterized using X-ray powder diffraction (XRD), Fourier transform infrared spectroscopy (FTIR), UV-Vis diffuse reflectance (DRS), thermo gravimetric analysis (TGA) and Raman spectroscopy. The as prepared samples have been used for the photocatalytic degradation of diethyl phthalate. Phthalate esters are one of the persistent organic pollutants found in the environment. Diethyl phthalate has been taken as a model pollutant. Zn doped TiO_2 sample shows better photocatalytic activity as compared to undoped TiO_2. The kinetic studies reveal that the photocatalytic degradation reaction follows a pseudo first order equation. The diethyl phthalate is almost completely degraded in about 200 min using 0.2 mol % Zn doped rutile TiO_2.

Keywords: Sol gel technique, Zn doped rutile TiO_2, Diethyl phthalate, Photocatalytic degradation

1 Introduction

Water pollution is one of the most serious threats faced on a global scale. The waste water of various industries, factories, laboratories etc. contains many organic pollutants. These are causing serious concern due to their continuous discharge into water and persistence. It has become a challenge to achieve the effective removal of persistent organic pollutants from waste water effluents. There is an urgent need to develop environmentally harmonious, ecologically safe and sustainable chemical technologies.

Phthalate esters are the most frequently detected persistent organic pollutants in the environment. Phthalate esters have been found in considerable quantities in river water, waste water, and drinking water. The US Environmental Protection Agency and the Chinese Environmental Monitoring Center has considered phthalate esters as priority water pollutants[1]. Due to relatively high boiling point and low melting point, phthalate esters are used as plasticizers, heat-transfer fluids and carriers in the polymer industry. Tons of phthalate esters are produced annually. These are used in flooring, paints, lubricants, wallpapers, toys, medical products, plastic packing films, electronic and auto products, personal care products, printing inks, special adhesive formulations, roofing system etc[2]. Phthalate esters have been considered as endocrine disrupting compounds. The studies on the animals confirmed the toxic effects of phthalate esters particularly mutagenic and teratogenic effects. Phthalate esters have adverse effects on male and female reproductive system[3]. When a phthalate ester is incorporated into a polymer matrix; it decreases the glass transition temperature of the polymer. Phthalate esters can easily migrate to surface of polymer matrix where they may be lost by a variety of physical processes because they are not bound to the polymer with covalent bonds[4].

There are many physical and biochemical methods available for the degradation of organic pollutants from waste water. Heterogeneous photocatalytic degradation is one of the most advantageous techniques due to complete mineralization, low cost, mild temperature and pressure conditions and no secondary pollution problems[5]. Titanium dioxide (TiO_2) is widely used to degrade many organic pollutants using heterogeneous photo catalytic degradation technique. TiO_2 has very good properties like stability, nontoxicity, less cost, environmental friendliness, strong oxidizing power, photocatalytic activity etc.[6,7]. TiO_2 has some limitations of wide band gap and high rate of electron hole recombination. Wide band gap of TiO_2 limits its use in UV region only and high electron hole

recombination decreases its photocatalytic efficiency[8]. Incorporation of transition metals into TiO_2 lattice by adding the transition metal salt as dopant source is an efficient method to overcome the limitations of TiO_2[9]. Transition metal dopants in TiO_2, extend the absorption region from UV to visible region by creating the defect sites. Moreover, transition metal dopants act as trapping sites to reduce the electron hole recombination. Thus, transition metals help in increasing the photo catalytic activity of TiO_2 invisible region of solar energy[10].

Many reports are available in literature, regarding the degradation of phthalate esters by many methods[11-14]. Very few reports are available in the literature related to the degradation of phthalate esters using TiO_2 based photocatalytic degradation[15-17]. To the best of our knowledge, there is no report related to the degradation of phthalate esters using Zn doped TiO_2.

The present study focuses on the synthesis of undoped and Zn doped TiO_2 by the sol gel method. Many researchers have doped Zn into TiO_2 by various processing methods to increase photocatalytic activity[18-22] of TiO_2. The synthesized photocatalysts are used to degrade diethyl phthalate ester.

2 Experimental Methods

2.1 Materials

In the present study, the chemicals used are titanium tetraisopropoxide (Sigma Aldrich, 97%), 2-propanol (Merck, 99.5%), zinc acetate (Rankem, 99.0%), hydrochloric acid (LobaChemie, 35%) and diethyl phthalate (Sd Fine Chem., 99.0%). All these chemicals are used in pristine form without any further purification. Doubly distilled water is used in all experiments.

2.2 Preparation of samples

Undoped and zinc doped TiO_2 samples were prepared by the sol gel method using titanium (IV) isopropoxide and zinc acetate as the precursors. In the first step of synthesis of undoped TiO_2, titanium tetraisopropoxide and isopropanol were mixed in molar ratio of 1:15. This solution was stirred for 30 min followed by ultrasonication of 10 min. In the second step of synthesis, a second solution was made containing water, isopropanol, hydrochloric acid in molar ratio of 1: 2.95: 0.545. After that, the solution made in the first step was added drop wise to second solution. A transparent color sol was obtained after complete addition which was magnetically stirred for

5 h to obtain the gel. This gel was kept for aging for 5 days. After that, the gel was dried at 100 °C. The dried solid was ground in an agate mortar to get a fine and uniform powder. In the end, the obtained powder was calcined at 450 °C for 2 . Zn doped TiO_2 sample was synthesized in a similar manner to the method described above except zinc acetate was added in second solution. The amount of zinc doped was 0.2 mol % relative to Ti. The above procedure for the synthesis of samples followed the work of Chen *et al.*[23].

2.3 Characterization of samples

The formation of different TiO_2 phases and crystallite sizes of samples were determined using X-ray diffraction (XRD) analyses performed on PANalytical's X'Pert Pro X-ray diffractometer (40 kV, 40 mA) using Cu Kα radiations (λ=1.54 Å). Samples were scanned over the angular range of 20°-80°. UV-Vis diffuse reflectance spectra (DRS) were performed to determine the optical absorption properties of samples using UV-Vis Spectrophotometer (Hitachi U-3900H) in spectral range of 250-800 nm. The sampling interval and scan speed during scan was 0.50 nm and 300 nm/min, respectively. FTIR patterns of the samples were recorded on FTIR spectrometer, Model RZX (Perkin Elmer) using KBr pellets in scan range of 4000 cm^{-1} to 250 cm^{-1}. The resolution of the FTIR instrument is 1 cm^{-1}. A NETZCH Zupiter STA 449 F3 simultaneous thermal analyzer was used to carry out thermal analysis of samples in argon atmosphere with heating rate of 10 °C/min from 25 to 800 °C. Raman spectra of samples were collected using Renishaw in Via Raman spectrometer. The photocatalytic activity of samples was studied by degradation of diethyl phthalate. The percentage degradation of diethyl phthalate was monitored by UV-Vis spectrophotometer (Hitachi U-3900H).

2.4 Photocatalytic degradation experiment

The photocatalytic degradation reaction was carried out in an immersion type photoreactor having three jackets with an effective volume of 100 mL. All the three jackets are made up of borosilicate glass. The aqueous suspension of diethyl phthalate and photocatalyst was filled in first jacket; second jacket was used for circulating water and a mercury lamp of 125 W having intensity 40,000 lux was placed axially in third jacket. More details about this reactor have been given in our previous publication[24]. The complete assembly was placed on the magnetic stirrer. At the start of experiment, the suspension was

magnetically stirred in dark for 30 min to get absorption desorption equilibrium. After that, during photoreaction, suspension was magnetically stirred continuously. The small part of the suspension was taken after regular intervals during photoreaction. To remove the photocatalyst, samples were filtered through Millipore syringe filter (PTFE, 0.45 μm). The absorption data of resulting samples, collected from UV-Vis spectrometer helps us to study the degradation of diethyl phthalateon the basis of Beer-Lambert Law.

3 Results and Discussion

3.1 XRD analysis

The X-ray diffraction patterns of undoped and Zn doped TiO_2 samples calcined at 450 °C are shown in Fig. 1. From the figure it is clear that there are two phases namely rutile [ICDD No. 01-089-0555] and brookite [ICDD No. 01-075-1582]. Rutile phase is found to be the predominant phase. Structurally, it is tetragonal belonging to P42/mm space group. The characteristic peaks of rutile and brookite are at 2θ of 27.45° (110) and 25.34° (210), respectively. The volume fractions of both the phases are calculated using direct comparison method[25]. Comparing the characteristic peak intensities of rutile (I_R, 27.45°) and brookite (I_B, 25.34°) peaks, I_R/I_B ratio is more in Zn doped TiO_2 as compared to the undoped sample. The volume fraction of rutile phase in undoped and 0.2 mol% Zn doped TiO_2 is 90% and 92%, respectively. The volume fraction of rutile phase is increasing in doped sample. In other words, the doping of zinc retards the formation of brookite in Zn doped TiO_2 sample. The crystallite size of undoped
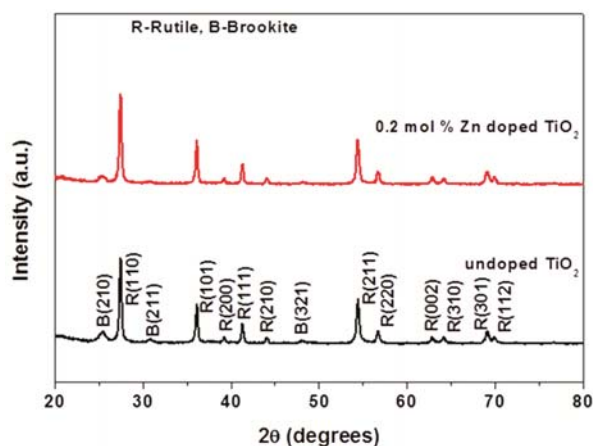
and Zn doped TiO_2 sample, estimated using Scherrer equation[26] is found to be around 27 nm. There is no characteristic peak corresponding to Zn. The absence of peaks due to metal may be attributed to fine dispersion of metal particles on TiO_2 or due to very small metal content[27].

3.2 UV-Vis analysis

Figure 2 shows the UV-Vis absorption spectrum of undoped and Zn doped TiO_2 sample. From figure, it is clear that in of case doped sample; there is considerable absorbance in range of 400-550 nm, as compared to undoped sample. This reveals that doping to zinc extends the absorption region of TiO_2 to visible region. It also indicates the creation of few electronic energy levels below the conduction band. However, density of these energy levels is low as indicated by the absorption in this spectral range. The band gap of the samples is calculated by Kubelka-Munk function[28,29]. The Kubelka-Munk function for diffuse reflectance is $f(R) = (1-R)^2/2R$, where R is the diffuse reflectance. To get band gap energy, $(f(R).hv)^{1/2}$ is plotted against hv as shown in Fig. 3. The band gap energy values of undoped and 0.2 mol% Zn-TiO_2 sample are 2.96 and 2.82, respectively. The red shift in doped samples is due to charge transitions between impurity bands and TiO_2 conduction band. Urbach energy is calculated by plotting ln $f(R)$ versus hv, taking the reciprocal of the linear portion, we get urbach energy[30]. The urabch energy of undoped and doped sample is found to be 0.064 eV and 0.099 eV, respectively. The more urbach energy in the doped sample shows the more disordering in doped sample as compared to undoped sample.
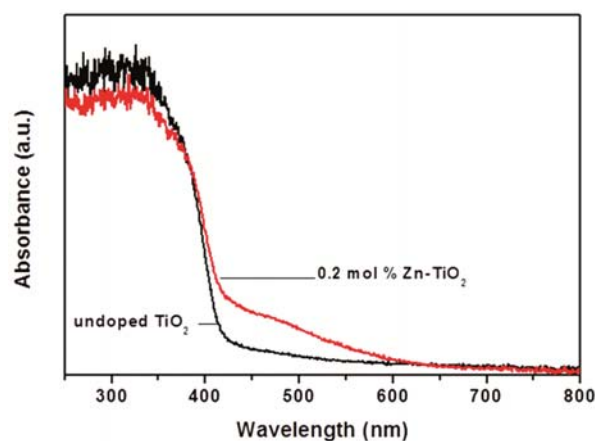

Fig. 1 — XRD patterns of undoped and Zn doped TiO_2 calcined at 450 °C.

Fig. 2 — UV-Vis absorption spectra of undoped and Zn doped TiO_2 calcined at 450 °C.

3.3 FTIR analysis

Figure 4 shows the FTIR spectra of undoped and Zn doped TiO_2 samples. The bands around 1620-1635 cm^{-1} correspond to the bending vibrations of surface adsorbed water molecules[31]. The bands around 3350-3450 cm^{-1} correspond to the stretching vibrations of OH groups[31,32]. The bands between 650 and 830 cm^{-1} correspond to different vibrational modes[33] of TiO_2. The strong bands around 667 cm^{-1} confirm the presence of rutile phase of TiO_2. IR spectra of rutile TiO_2 are characterized by a broad band with transmittance minima[34] at 722, 590, 525 and 471 cm^{-1}. It is clear that the band around 667 cm^{-1} is more intense and broad in doped sample as compared to undoped sample due to modification.

3.4 Raman analysis

Figure 5 shows the Raman spectra of undoped and Zn doped TiO_2 sample. The unit cell of the rutile titania structure having space group D_4H^{14}
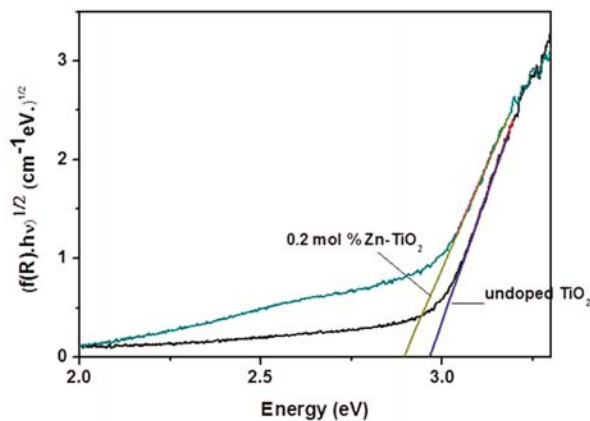
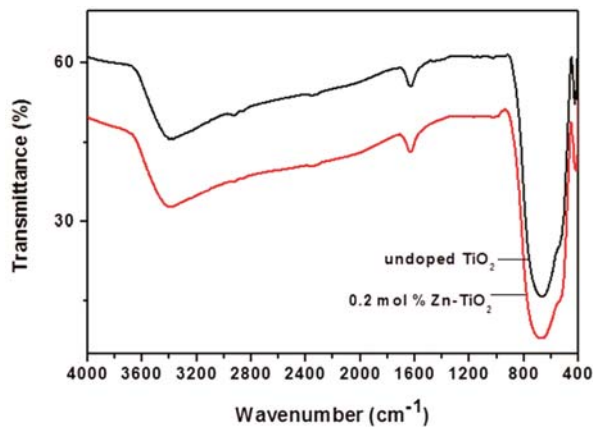Fig. 3 — Determination of band gap using Kubelka-Munk function.

Fig. 4 — FTIR patterns of undoped and Zn doped TiO_2 calcined at 450 °C.

(P42/mnm) contains two TiO_2 molecules in the unit cell. From a group theory analysis, it can be shown that 15 fundamental modes haves the following irreducible representations[33]: A1g + A2g + A2u + B1g + B2g+ 2 B1u + Eg +3 Eu. Further, A1g + B1g + B2g + Eg are Raman active and four modes A2u + 3Eu are infrared active. The other three modes A2g + 2 B1u are neither Raman active nor infrared active[34]. For rutile TiO_2, there are four Raman active modes[35] at 144 (B1g), 448 (Eg), 613 (Ag) and 827 (B2g) cm^{-1}. Brookite has three Raman bands[20] at 366, 326 and 247 cm^{-1}. In our results the weak bands at 247, 326, 366 cm^{-1} are due to brookite phase of TiO_2. B1g mode comes from the stretching of Ti-O bonds which is a dominant mode in above spectra[35]. Raman spectra of our samples show appearance of characteristic bands at 148, 444 and 610 cm^{-1} which is attributed to the B1g, Eg, Ag modes of rutile TiO_2, respectively. Raman spectra of our samples are consistent with XRD data which show presence of rutile phase as major phase of TiO_2. The Raman band around 1640 cm^{-1} is due to surface absorbed water molecules. The band is more intense and broad in Zn doped sample as compared to the undoped showing the presence of more surface adsorbed water molecules in doped sample as compared to undoped sample. This accounts for the higher photocatalytic activity of doped sample as compared to undoped sample.

3.5 TGA analysis

Figure 6 shows thermogravimetric curves of undoped and Zn doped TiO_2 samples. Thermogravimetric measurements show that both the samples undergo weight loss with increase in temperature. The weight loss is more in undoped sample as compared to doped sample which reveals about greater thermal stability of doped sample as
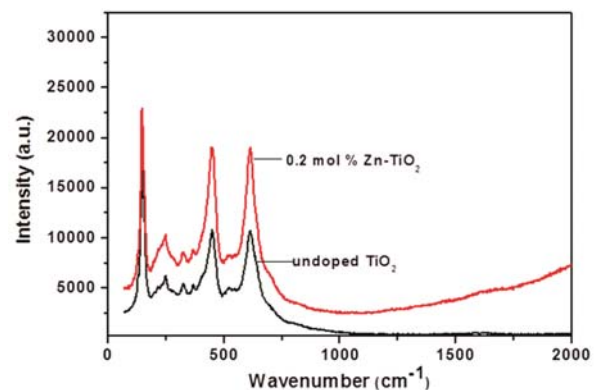
Fig. 5 — Raman spectra of undoped and Zn doped TiO_2 samples.

compared to undoped sample. The curve below 100 °C in TGA of both sample show desorption or drying. This is due to loss of adsorbed water molecules on surface. Both samples show mass loss occurs mainly up to 550 °C.

3.6 Photocatalytic activity

The photocatalytic activity of undoped and Zn doped TiO_2 sample is determined in terms of photocatalytic degradation of diethyl phthalate. Diethyl phthalate consists of a benzene ring with two carboxylic acid ethyl esters attached to it in the ortho position (as shown in Fig. 7). It is a highly conjugated system, as the pi-cloud on the benzene ring, the p-orbitals on the carbonyl atoms and the lone pairs on the oxygens are all conjugated. The substituents are meta-directing and they are ortho to each other, so all positions in the ring are more or less equally deactivated[36]. Due to conjugation, it is a stable compound and difficult to degrade. In UV-Vis spectrum of diethyl phthalate, there are two intense bands at wavelengths of 229 nm and 276 nm. An aqueous solution of diethyl phthalate was irradiated with high pressure mercury lamp in presence of undoped and Zn doped TiO_2 samples.
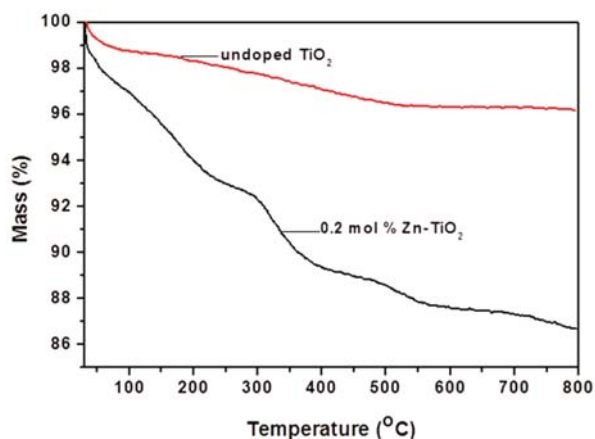
From Fig. 8, it is clear that absorption peak at λ_{max}= 229 nm is diminishing with time during irradiation which reveals the degradation of diethyl phthalate. Kinetic studies have been done in order to have a better comparison of photocatalytic efficiencies of the samples.

Figure 9 shows the plot of ln (C_o/C) versus irradiation time. The results show that degradation of diethyl phthalate for both the samples, follows the pseudo first order kinetics model, ln $(C_o/C) = k_{app}t$, where C is the concentration of diethyl phthalate at time t, C_o is the initial concentration of diethyl phthalate, k_{app} is the apparent first order rate constant[37] (min^{-1}). k_{app} is derived from ln (C_o/C) versus t plots. The k_{app} value for undoped and Zn doped TiO_2 sample is found to be 0.0059 min^{-1} and 0.010 min^{-1}. The k_{pp} value for doped sample is more than undoped sample
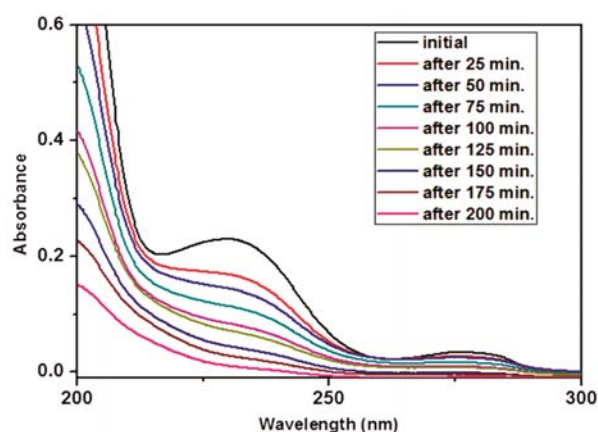

Fig. 8 — Degradation of diethyl phthalate during light irradiation in presence of 0.2 mol% Zn-TiO_2 when C_o = 30 ppm, catalyst load = 1 g/l.

Fig. 6 — Thermo gravimetric curves of undoped and Zn doped TiO_2.

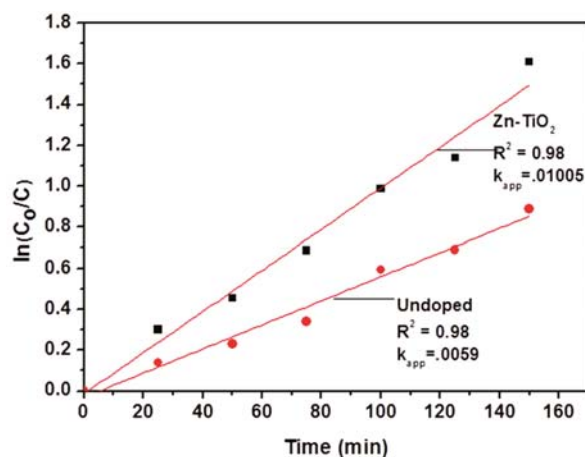Fig. 7 — Chemical structure of diethyl phthalate.

Fig. 9 — Kinetic study of photocatalytic degradation of diethyl phthalate using undoped and Zn doped TiO_2.

which reveals the higher photcatalytic efficiency of doped sample.

4 Conclusions

Undoped and Zn doped TiO_2 samples are synthesized using sol gel technique. X-ray diffraction study confirms that the samples are predominantly in rutile phase. Moreover, the doping of zinc retards the formation of brookite phase. Raman spectra of samples support the observation of X-ray diffraction patterns that the samples are predominantly in rutile phase. Doping of zinc causes the red shift in the sample. Thermal analysis reveals that doped sample is more thermally stable than undoped TiO_2. Zn doped TiO_2 sample has more photocatalytic efficiency than undoped sample.

Acknowledgement

References

1 Gao D W & Wen Z D, *Sci Total Environ*, 541 (2016) 986.
2 Abdel daiem M M, Rivera-Utrilla J, Ocampo-Perez R, Mendez Diaz J D & Sanchez-Polo M, *J Environ Manage*, 109 (2012) 164.
3 Jinling Y, Yongxin L, Yu W, Ruan J, Zhang J & Sun C, *Trends Analyt Chem*, 72 (2015) 10.
4 Staples C A, Phthalate esters: *The handbook of environmental chemistry*, (Springer-Verlag: Berlin Heidelberg), 2003.
5 Chong M N, Jin B, Chow C W & Saint C, *Water Res*, 44 (2010) 2997.
6 Suwanchawalit C, Wongnawa S, Sriprang P & Meanha P, *Ceram Int*, 38 (2012) 5201.
7 Liu W, Chen S, Zhao W & Zhang S, *Desalination*, 249 (2009) 1288.
8 Wang S, Lian J S, Zheng W T & Jiang Q, *Appl Surf Sci*, 263 (2012) 260.
9 Wang S, Bai L N, Sun H M, Jiang Q & Lian J S, *Powder Technol*, 244 (2013) 9.
10 Kerkez-Kuyumcua O, Kibarb E, Dayıogluc K, Gedikc F, Akın A N & Ozkara-Aydinoglua S J, *Photochem Photobiol A Chem*, 311 (2015) 176.
11 Xu L J, Chu W & Graham N, *Ultrason Sonochem*, 20 (2013) 892.
12 Sarkar J, Chowdhury P P & Dutta T K, *Chemosphere*, 90 (2013) 2571.
13 Wu Q, Liu H, Ye L S & Wang Y H, *Int Biodeterior Biodegradation*, 76 (2013) 102.
14 He Z, Xiao H, Tang L, Min H & Lu Z, *Bioresour Technol*, 128 (2013) 526.
15 Jiana W, Joensa J A, Dionysioub D D & O'Sheaa K E, *J Photochem Photobiol A Chem*, 262 (2013) 7.
16 Jing Y, Li L, Zhang Q, Lu P, Liu P & Lu X, *J Hazard Mater*, 189 (2011) 40.
17 Ding X, An T, Li G, Chen J, Sheng G, Fu J & Zhao, *J Res Chem Intermediat*, 34 (2008) 63.
18 Zhang W, Zhu S, Lib Y & Wang F, *Vacuum*, 82 (2008) 328.
19 Suwanboon S, Amornpitoksuk P & Bangrak P, *Ceram Int*, 37 (2011) 333.
20 Devi L G, Murthy B N & Kumar S G, *Mater Sci Eng B*, 166 (2010) 1.
21 Chauhan R, Kumar A & Chaudhary R, *J Sol-Gel Sci Technol*, 61 (2012) 585.
22 Singla P, Sharma M, Pandey O P & Singh K, *Appl Phys A*, 116 (2014) 371.
23 Chen C, Wang Z, Ruan S, Zhao M, Zou B & Wu F, *Dyes Pigments*, 77 (2008) 204.
24 Singla P, Pandey O P & Singh K, *Int J Environ Sci Technol*, 13 (2016) 849.
25 Cullity B D & Stock S R, *Elements of X-ray Diffraction* (Prestine Hall, USA) (2001).
26 Umar K, Haque M M, Muneer M, Harada T & Matsumura M, *J Alloys Compd*, 578 (2013) 431.
27 Vijayan P, Mahendiran C, Suresh C & Shanthi K, *Catal Today*, 141 (2009) 220.
28 Gambhire A B, Lande M K, Arbad B R, Rathod S B, Gholap R S & Patil K R, *Mater Chem Phys*, 125 (2011) 807.
29 Aguilar T, Navas J, Alcantara R, Lorenzo C F, Gallardo J, Blanco G & Calleja J M, *Chem Phys Lett*, 571 (2013) 49.
30 Singh S & Singh K, *J Non Cryst Solids*, 386 (2014) 100.
31 Venkatachalam N, Palanichamy M & Murugesan V, *J Mol Catal A Chem*, 273 (2007) 177.
32 Ghasemi S, Rahimnejad S, Setayesh S R, Rohani S & Gholami M R, *J Hazard Mater*, 172 (2009) 1573.
33 Ganesh I, Gupta A K, Kumar P P, Sekhar P S C, Radha K, Padmanabham G & Sundararajan G, *Sci World J*, 2012 (2012) 1.
34 Bezrodna T, Gavrilko T, Puchkovska G, Baran J & Marchewka M, *J Mol Struct*, 614 (2002) 315.
35 Shen H, Mi L, Xu P, Shen W & Wang P N, *Appl Surf Sci*, 253 (2007) 7024.
36 Maitland J, *Organic chemistry*, (W W Nortan & Company: New York), 2001.
37 Yue X, Jin X, Wang R, Ni L, Jiang S & Qiu S, *Mater Chem Phys*, 161 (2016) 162.